AIAA JOURNAL
Vol. 43, No. 5, May 2005

Key Links in Space Weather: Forecasting Solar-Generated Shocks and Proton Acceleration

C. D. Fry*
Exploration Physics International, Inc., Huntsville, Alabama 35806
M. Dryer†
National Oceanic and Atmospheric Administration, Boulder, Colorado 80305
W. Sun‡ and C. S. Deehr§
University of Alaska, Fairbanks, Alaska 99775
Z. Smith¶ and T. R. Detman**
National Oceanic and Atmospheric Administration, Boulder, Colorado 80305
A. Aran††
Institut d'Estudis Espacials de Catalunya, E-08034 Barcelona, Spain
D. Lario‡‡
Johns Hopkins University, Applied Physics Laboratory, Laurel, Maryland 20723
B. Sanahuja§§
Universitat de Barcelona, E-08028 Barcelona, Spain
and
S.-I. Akasofu¶¶
University of Alaska, Fairbanks, Alaska 99773

Forecasting the arrival of solar-generated shocks and accelerated protons anywhere in the heliosphere presents an awesome challenge in the new field of space weather. Currently, observations of solar wind plasmas and interplanetary magnetic fields are made at the sun–Earth libration point, L1, about 0.01 astronomical units (∼245 Earth radii) sunward of our planet. An obvious analogy is the pitot tube that protrudes ahead of a supersonic vehicle. The Advanced Composition Explorer and Solar and Heliospheric Observatory spacecraft, currently performing this function, provide about $\frac{1}{2}$–1 h advance notice of impending arrival of interplanetary disturbances. The signatures of these disturbances may be manifested as interplanetary shock waves and/or coronal mass ejecta. We describe a first-generation procedure, based on first-principles numerical modeling, that provides the key links required to increase the advance notice (or lead time) to days, or even weeks. This procedure, instituted at the start of the present solar cycle 23, involves three separate models, used in real time, to predict the arrival of solar-event-initiated interplanetary shock waves at the L1 location. We present statistical results, using L1 observations as "ground truth" for 380 events. We also briefly discuss how one of these models (Hakamada–Akasofu–Fry version 2) may be used with a model that predicts the flux and fluence of energetic particles, for energies up to 100 MeV, that are generated by these propagating interplanetary shock waves.

I. Introduction

GEOMAGNETIC storms and proton radiation hazards are two of the panoply of space weather concerns for modern technology and human activities (cf. the National Academy of Sciences Decadal Study[1]). We believe that they are amenable to fluid mechanics efforts. We take the view that some energetic solar flares generate fast coronal mass ejections (CMEs), which, in turn, generate shocks. These latter combinations, called interplanetary coronal mass ejections (ICMEs), interact with the Earth's magnetosphere, spacecraft en route to Mars, and even the Martian environment itself. If the magnitude and polarity of the interplanetary magnetic field (IMF) became large and southward, a geomagnetic storm would take place at Earth within hours after shock impact. Prior to this initiating "storm sudden commencement," indeed, beginning at the solar initiating source, the shock becomes an accelerator of protons (and also of heavier species that are not considered here) that spiral along the IMF outward toward Earth, possibly to Mars, and to outward-bound spacecraft.

The forecasters' objective is to predict the shock's arrival time and, thereafter, the temporal profile of the polarity and magnitude of the IMF, as well as the flux and fluence of the shock-accelerated protons. A complementary scientific objective is the prediction of other solar wind properties such as density and temperature; however, these properties are of secondary concern to the operational goals of the space weather forecasters.

Presented as Paper 2003-1226 at the AIAA Aerospace Sciences Meeting, Reno, NV, 6–9 January 2003; received 11 June 2004; revision received 14 October 2004; accepted for publication 26 October 2004.

*Vice President, 6275 University Drive, Suite 37-105; gfry@expi.com. Member AIAA.
†Scientist Emeritus, Space Environment Center; also Scientist Emeritus, Exploration Physics International, Inc., Huntsville, AL 35806; Murray.Dryer@noaa.gov. Associate Fellow AIAA, Retired.
‡Research Scientist, Geophysical Institute; sun@jupiter.gi.alaska.edu.
§Professor of Physics, Emeritus, Geophysical Institute; cdeehr@gi.alaska.edu.
¶Physicist, Space Environment Center; Zdenka.Smith@noaa.gov.
**Physicist, Space Environment Center; Thomas.R.Detman@noaa.gov.
††Ph.D. Candidate; also Ph.D. Candidate, Departament Astronomia i Meteorologia, Universitat de Barcelona, E-08028 Barcelona, Spain; aaran@am.ub.es.
‡‡NRC Senior Research Associate; David.Lario@jhuapl.edu.
§§Dean of Sciences, Departament Astronomia i Meteorologia; blai@am.ub.es.
¶¶Director, International Arctic Research Center; sakasofu@iarc.uaf.edu.

We will describe the present status of an operational forecasting system that provides, first, 28-day predictions of solar wind speeds and shocks from corotating, high-speed, coronal hole streams. We refer to these temporal profiles at Earth, and elsewhere in the ecliptic plane, as "nonevents" because their objective is to describe the nonhomogeneous background solar wind flow. Second, the output also incorporates solar disturbances, or "events," which, in many cases, are associated with the shock-led ICMEs that run into and over the nonevent flows.

The input data to the system for the events are characterized by 1) solar activity location, as provided by optical U.S. Air Force (USAF) H_α (656.3-nm) flare observations; 2) energy output indirectly provided by the proxy coronal shock speed, as estimated by the metric radio Type II's temporal drift in plasma frequency with the use of a coronal density model; and 3) the piston driving time, as suggested by the proxy duration of the National Oceanic and Atmospheric Administration (NOAA)/Geostationary Operational Environmental Satellite (GOES) spacecraft's soft x-ray enhancement due to the flare. For these calculations an "event" is identified as coincident with ($\ll\frac{1}{2}$ h) optical and x-ray flare and metric Type II radio burst observations. Thus, the flare provides the approximate location for the initial pulse for models such as those discussed here.

The 20-year background for this methodology (i.e., several versions of the Hakamada–Akasofu–Fry model, the latest being HAFv.2) is described by Akasofu[2] and Fry et al.[3] Eventually, HAFv.2 will form part of, or even be replaced by, a hybrid system that includes the HAF (version 3) model and a first-principles three-dimensional MHD model as envisioned by Dryer[4,5] and T. R. Detman (NOAA Space Environment Center, private communication, 2004).

HAFv.2's kinematic procedure follows fluid parcels and frozen-in IMF field lines. This approach to first principles conserves mass and momentum but not energy. Its internal parameters have been calibrated with a one-dimensional MHD model.[4,6] We will describe HAFv.2's experience as part of a real-time ensemble experiment with two other models: STOA (shock time of arrival, based on self-similarity, strong shock, blast wave theory) and ISPM (interplanetary shock propagation model, based on a parameterized set of numerical experiments with a two-dimensional MHD model). Early successful use of the STOA model (Manoharan et al.[7]; Janardhan et al.[8]) was demonstrated, together with interplanetary scintillation observations, in the tracking of interplanetary shocks through space. The two latter models use only a uniform background solar wind and cannot handle multiple events that interact because they are closely spaced in time or location. These models, moreover, do not include the nonhomogeneity of the background flow, nor do they have the ability to consider interacting events that are closely spaced in time. HAFv.2, on the other hand, has no such restrictions. AIAA fluid mechanics experts will recognize the "event" analog as a transparent reference to a shock tube, where the diaphragm's puncture is an approximation to the complex reconnection physics considered to be the source of the shock energy at, or close to, the solar photosphere.

In this paper, we propose the logical extension of the model discussed above to large gradual solar energetic particle events (SEPs) and energetic storm particle events (ESPs) that pose a threat to humans, spacecraft components, and operations. Examples of such events, combined with the real-time forecast experiment noted above, are given by McKenna-Lawlor et al.[9] Lario et al.[10] (and references therein) moved from the fluid continuum approximation described above to the particle physics regime. We adopted the two-dimensional MHD code and used the shock jump conditions at each point on the expanding shock wave. With a parameterized set of shocks (various solar flare locations relative to the observer, varying initial coronal shock speeds, and several piston driving times), we examined the shock connection with the observer along the IMF. That is, we empirically determined the injection of shock-accelerated proton flux, for energies up to 100 MeV, from the moving point along the shock front that connects to the observer. Thus, we coined the acronym COBpoint (connection with observer point). Using a realistic simulation of the particle transport from the COBpoint and along the IMF as the shock expands throughout the heliosphere, we successfully modeled the flux of particles measured at several spacecraft. Sanahuja et al.[11] and Aran et al.[12] utilized these studies to develop an operational model for the prediction of proton flux and fluence up to energies of 8 MeV at solar distances of 0.4 and 1 astronomical units (AU).

In Sec. II, we briefly describe the input and output of the HAFv.2 model associated with a geoeffective event during the interval 4–7 November 2001. We also summarize our seminal real-time forecasting experience with 380 events during solar cycle 23. In Sec. III, we sketch the potential use of the HAFv.2 model to predict the flux and fluence of energetic particles from propagating interplanetary shock waves via the COBpoint approach. Finally, we add some concluding remarks in Sec. IV.

II. Real-Time Examples of HAFv.2 Shock Forecasting and Statistical Results

The first key link in our space weather forecasting system is to describe the solar wind and IMF under both quiet and disturbed conditions at the sun. It is imperative that a quiescent background, albeit nonhomogeneous and time-varying, be established for the heliospheric flow of these conditions. Input for this nonevent background is provided by solar surface magnetograms (from the National Solar Observatory, Tucson, Arizona), which are utilized to construct a potential field coronal magnetic field model, the so-called hairy billiard ball. This model is then used to build a map of the radial IMF and velocity[13,14] at a spherical source surface at 2.5 R_S (where $R_S =$ solar radius $= 6.9 \times 10^5$ km). These inner boundary conditions are then used to initialize the kinematic HAFv.2 code.[3,15]

The second key link, the interplanetary background solar wind plasma and magnetic field IMF, is established as follows. The HAFv.2 model is run, and the results are calculations of the solar wind conditions from the sun to the Earth and beyond. The output of the HAFv.2 model has been extended to beyond 10 AU but is routinely confined to 2 AU for prediction purposes associated with the terrestrial planets. These results provide a simulation of fast and slow solar wind streams together with both inward and outward IMF polarity in the ecliptic plane. This nonuniform background includes corotating coronal hole flow interactions as well as the deformed heliospheric current sheet. It is updated whenever new source surface maps become available, currently daily. This procedure simulates the varying flow of the nonevent plasma and IMF past the Earth and the other planets. The passage of large-magnitude, southerly-directed IMF structures (approximately $B_z =$ 10 nT for about 3 h or more) under such conditions can, in its own right, be geoeffective by generating geomagnetic activity.

Events such as flares, eruptive prominences, and destabilized helmet streamers constitute an obvious "modification" to this second key link in the chain that leads to Earth (Mars, etc.). The best way to mimic these solar events is currently an area of intense discussion and, often, controversy in the face of limited solar observations and diagnostics. We have chosen to focus on the solar flare and its associated metric type II radio emission. The flare is accompanied by a variety of immediate particle and electromagnetic emissions. The metric type II radio burst starts at or near the time of maximum soft x-ray emission. This radio burst drifts downward in frequency, f, with time. It is caused by electron oscillations at the fundamental and higher harmonics of the plasma frequency. The first harmonic is proportional to the square root of the local electron density, n, which decreases exponentially with height above the photosphere. The shock caused by the event is assumed to be the outward-moving agent for this electron oscillation and downward drift in frequency. The radio observation, coupled with a coronal density model, provides the initial coronal shock speed, V_S, the magnitude of which is related, via self-similarity theory, to the solar disturbance's energy output. This physically derived parameter, together with the duration of the flare's soft x-ray output, which serves as a proxy for the shock's piston-driving time, provides part of the initialization for the HAFv.2 model at the source surface (2.5 R_S). Optical (and/or x-ray imaged) observations of the flare provide the location on the solar disk of the source of the "event" energy output. These optical, radio, and x-ray observations are provided on a real-time basis by the USAF's Air Force Weather Agency and NOAA's Space Environment Center.

The forecaster can examine an ecliptic plane figure provided by HAFv.2 that shows the corotating flow and IMF during the "pre-event" specification of plasma and IMF background. Following the "event," the forecaster can examine the temporal and spatial evolution of the propagating interplanetary coronal mass ejection (ICME) together with its shock. An example is shown in Fig. 1: the predicted IMF configuration and the locations of Earth and Mars in the ecliptic plane at 12-h intervals during 4–7 November 2001. A long-duration flare took place on 4 November in NOAA active region 9684, located at solar coordinates N 02° W 23°. This flare was classified as X1.0 from its soft-x-ray signature and 3B by its optical H_α observation. GOES-8 at geosyncronous orbit detected the x-ray event maximum at 1620 UT, and the Holloman AFB solar observatory reported that the optical flare peaked at 1622 UT. Holloman also detected a metric type II radio burst beginning at 1610 UT (at a frequency of 180 MHz) and ending at 1621 UT (at 29 MHz) with an estimated coronal shock speed $V_S = 1329$ km/s. Preliminary estimates in real time of the SOHO/LASCO white light imagery suggested a fast halo CME. We assumed (in real time, on the basis of the duration of the proxy soft-x-ray emission enhancement) that a shock would be generated with a piston driving time $\tau =$ 1 h 45 min. The SWEPAM instrument on the Advanced Composition Explorer (ACE) spacecraft was, at that time, measuring a background solar wind speed $V_{SW} = 320$ km/s at the spacecraft's location at the sun–Earth libration point, L1.

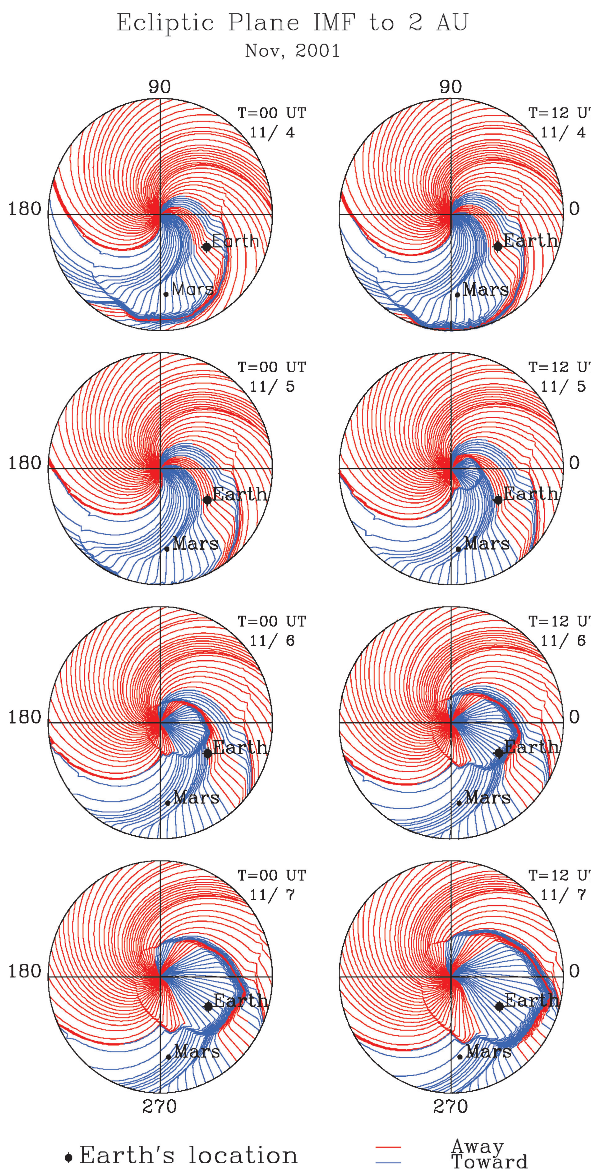

Fig. 1 Ecliptic plane showing the IMF polarity (red: directed away from the sun; blue: directed toward the sun) out to 2 AU as simulated by the HAFv.2 model. The period 0000 UT on 4 November 2001–1200 UT on 7 November 2001 is depicted in 12-h increments from top to bottom. Two propagating shocks are shown. The first shock is associated with a flare on 29 October at N12°E25° at 1113 UT (type II start); its far western flank was predicted to arrive on 3 November but, in reality, was much weaker than expected. The second, stronger shock is associated with the solar activity that took place on 4 November, as discussed in the text.

Figure 2 shows the physical parameters predicted by the HAFv.2 model and observed by ACE/SWEPAM at L1 during both the nonevent and event episodes. The signature of the latter is signaled by a sudden departure from the nonevent curve, that is, the arrival of the shock at this location. The predicted shock arrival time (SAT) is determined by computing a shock searching index (SSI). The SSI is equal to the logarithm (base 10) of the model's dynamic pressure change, normalized to the predisturbed dynamic pressure, at each time step. The event's SAT is predicted when this SSI reaches an empirically determined threshold value (currently SSI $= -0.35$). It is important to note that this forecast is usually made several days prior to the time of the jump in Fig. 2. If this SSI threshold is not achieved, the shock is declared to have decayed to an MHD wave by the time the disturbance reached the Earth's location. The error in timing is then the time difference ΔT_{HAF} (prediction time minus the observed SAT) obtained by comparing HAFv.2 model results with ACE and/or SOHO observations. Predicted SAT, when compared with ACE spacecraft observations, provides a metric for evaluating model performance and demonstrates the goodness of the temporal profiles of solar wind parameters modeled by HAFv.2.

Our group has pursued a unique, real-time SAT forecasting experiment since February 1997, near the beginning of the present solar cycle 23. The first phase included a study of 173 cases (February 1997–October 2000) that were described by Fry et al.[16] and Dryer.[17] The second phase included a study of 207 cases (October 2000–September 2002). This study focused upon predicting the SAT and not on any of the specific physical parameters such as plasma velocity V, IMF magnitude and polarity, $\boldsymbol{B}$ and in particular B_z, and density n.

Table 1 shows the contingency tables for the first phase of the study, during which HAFv.2 was tuned and the SSI threshold value noted above was established. HAFv.2 model results are compared with those produced by STOA and ISPM, as described by Fry et al.[16] and Dryer.[17] The rms error for the hits, determined using ΔT_{HAF} within ±24 h, was ~12 h. The Heidke skill score, which corrects for the probability of detecting a shock by chance, was 30% for the HAFv.2 model, about the same as in the other models. It should also be noted that successes (sum of 48 hits and 64 correct nulls) exceed failures (sum of 41 false alarms and 20 misses) by a 2:1 factor. Thus, the success rate (112/173) for HAFv.2 was 64.7%.

Table 2 shows the contingency table for HAFv.2 (after the SSI tuning mentioned earlier for the second phase of the study) and the other two models.

Table 1 Forecast contingency tables for the phase 1 tuning study

	Forecast		STOA prediction		ISPM prediction		HAFv.2 prediction	
Observation	Yes	No	Yes	No	Yes	No	Yes	No
Yes	a	b	53	15	39	29	48	20
No	c	d	57	48	31	74	41	64
Total	a + c	b + d	110	63	70	103	89	84

Table 2 Contingency tables for the second phase of the real-time SAT forecasting study

	Forecast		STOA prediction		ISPM prediction		HAFv.2 prediction	
Observation	Yes	No	Yes	No	Yes	No	Yes	No
Yes	a	b	84	32	71	45	77	39
No	c	d	52	39	25	66	40	51
Total	a + c	b + d	136	71	96	111	117	90

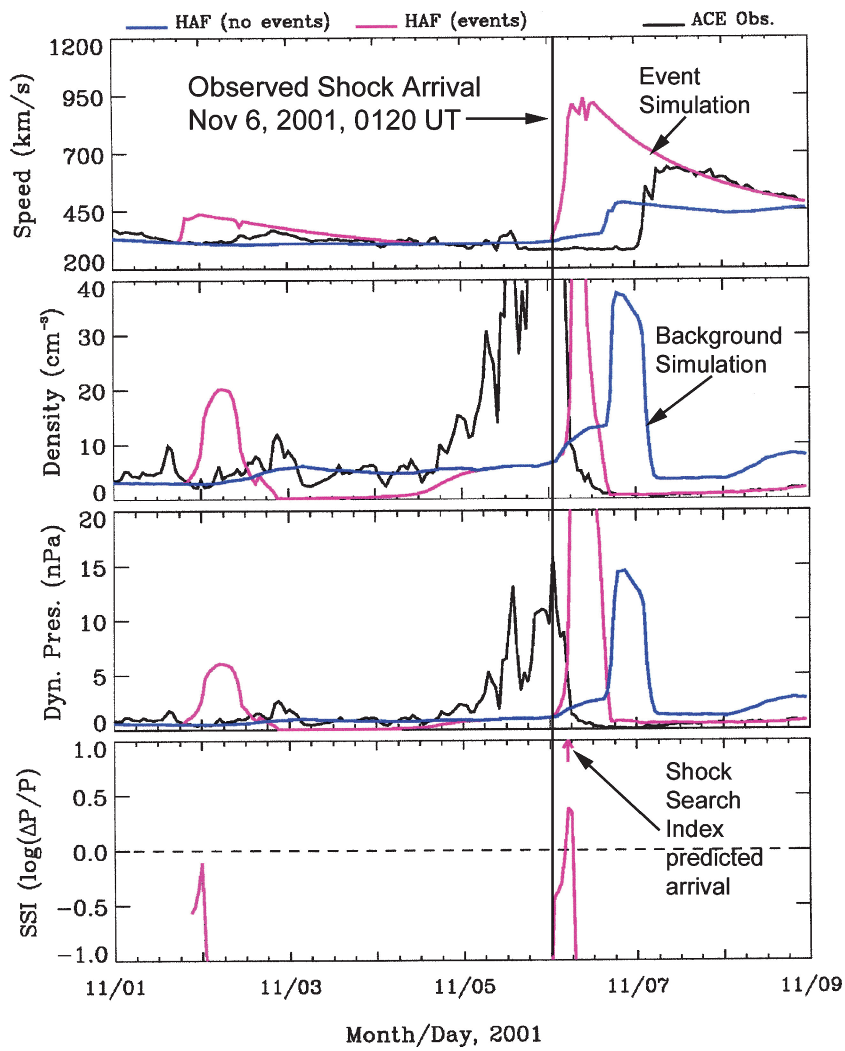

Fig. 2 Time series of solar wind speed, density, dynamic pressure, and shock searching index (see text) from 1 to 9 November 2001 at the L1 position. The blue curve is the simulated nonhomogeneous background solar wind flow, which is based on nonuniform conditions on the sun due to coronal holes and corotating fast and slow interacting solar wind streams. The red curve is the simulated response caused at L1 by the two flares noted in the legend for Fig. 1. The black curves are the real-time (level 1) ACE/SWEPAM data. We show these data, rather than the reconstructed level 2 data, to show the dropout of velocity data during the 5–6 November period. These dropouts were caused by the largest energetic proton flux (see Fig. 3) since the famous Bastille Day flare of 14 July 2000.[14] The actual shock arrival was recorded by the ACE/MAG magnetometer (which was unaffected by the energetic particles) at ∼0120 UT on 6 November 2001. The HAFv.2 prediction was for 3.6 h later.

This is a preliminary result because a rigorous check of the visualized ACE shocks, using Rankine–Hugoniot conditions, has yet to be made. At this point, however, we can say that the rms error remained at about 12 h for the HAFv.2 model. The Heidke skill score was reduced to 22% (compared to 30% in the first phase study) and probably reflects the more complicated physics during this active period of the solar cycle. Nevertheless, the successes (128 cases) still exceeded the failures (79 cases) for HAFv.2, with a slight success rate decrease to 61%.

The HAFv.2 model is therefore similar to the other models in its ability to predict the SAT. The advantage of HAFv.2 over the others, however, is its ability to describe the distorted solar wind due to multiple, interacting solar events and to separate shocks from corotating solar wind structures with similar signatures.

III. Energetic Particle Prediction: COBpoint Approach

The COBpoint was briefly defined in Sec. I. Our interpretation is that there is one COBpoint for each observer (spacecraft or planet), one point of which is at the root of the IMF line connecting the shock front with the spacecraft. This COBpoint changes with time as the shock propagates and expands, moving along the shock front. Figure 1 is a typical example, showing the interplanetary shock in the ecliptic plane, the location of the Earth, and the geometry of the IMF lines. Here, the COBpoint is the point on the front of the evolving shock that connects to the observer (in this case, Earth) along the IMF line at a given time. A similar exercise can obviously be made for an observer on Mars or for a spacecraft en route to that or any other planet.

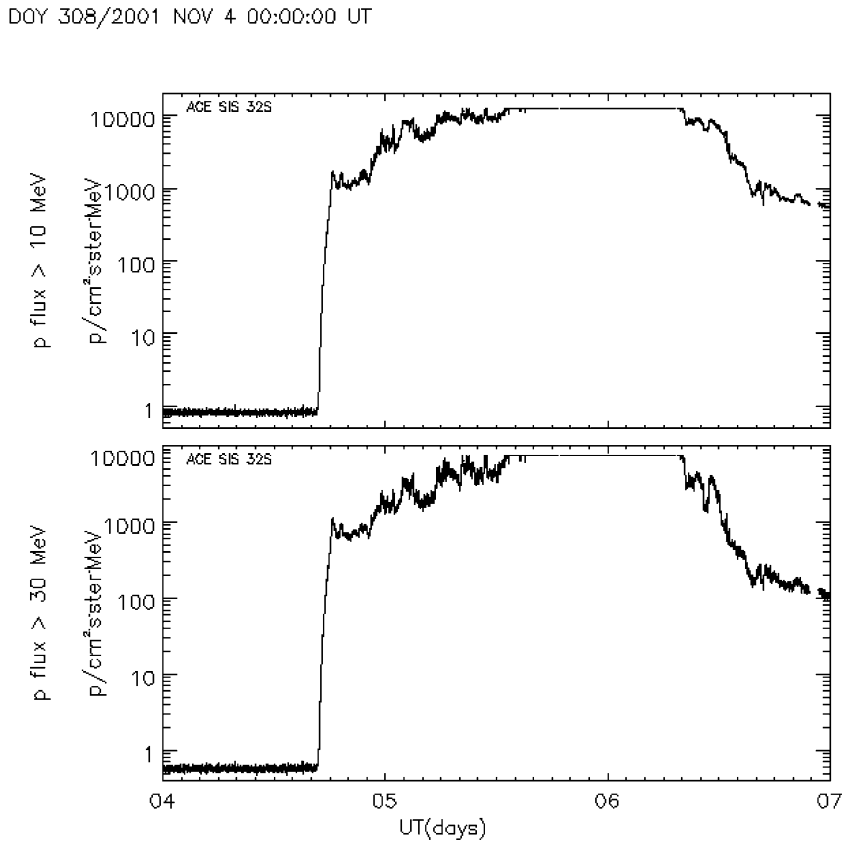

Fig. 3 Energetic proton flux (32 s resolution) measured as a consequence of both prompt arrival from the 4 November 2001 solar flare and the locally shock-energized process during its propagation, as simulated in Fig. 1. The upper panel is for proton flux >10 MeV, and the lower panel for proton flux >30 MeV. Note the off-scale response from midday on 5 November until early on 6 November, at which point the ACE/SWEPAM recovered its level 1 velocity data reception. Level 2 data for the >10 MeV proton intensities were later recovered (URLs http://www.srl.caltech.edu/ACE/ACENews/ACENews57.html). Parenthetically, we note that the full range 4 MeV < E < 500 MeV was received in real time by the GOES-8 spacecraft. Our objective here is to show that some scientific instruments, configured for real-time reception, may sometimes not respond properly under such energetic particle "snowstorm" conditions.

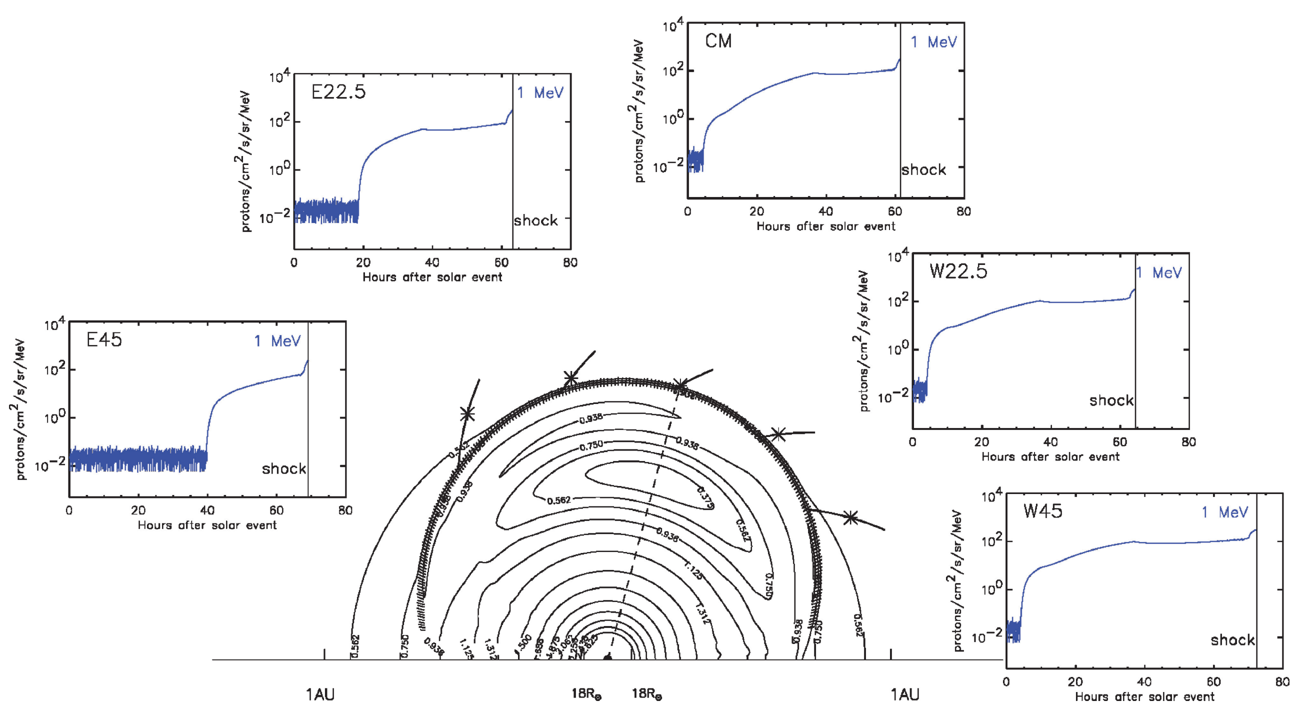

Fig. 4 Simulated energetic-particle response (1 MeV) associated with a CME and its triggered interplanetary shock (shown in the ecliptic plane). The shock, with contours of solar wind density, is from a two-dimensional MHD numerical simulation.[10] The middle, smaller panel is the response expected from an observer, such as at Earth at the flare's central meridian (CM). The other panels indicate the response from hypothetical observers located both east and west of the flare's CM. Note the much longer delay for particle flux response through the IMF connection from the COBpoint to the observer's position when the observer is located to the west of the flare's CM, that is, when the flare is at E45° relative to an Earth observer (from Aran et al.[12]).

The 4 November 2001 event is a dramatic example of energetic particle arrival at Earth following a flare, x-ray event, and metric type II radio burst (coincident in time within $\frac{1}{2}$ h of each other). Figure 3 shows the ACE/SIS instrument response for particles within two ranges of proton energies: >10 and >30 MeV. Our assessment of this event was as follows: the flare/CME/shock energization phase led to an immediate increase in ACE/SIS particle flux by at least three orders of magnitude. This was followed by continued enhanced flux within these energy ranges that reflected in situ energization at the COBpoint in the evolving shock as the shock propagated into the interplanetary medium. This process continued for more than 2 days after the onset of the solar activity, with variable efficiency as the shock moved outward. The additional fluence was enhanced still further by the sudden energetic storm particle (ESP) increase within all channels when the shock arrived at Earth at ~0120 UT on 6 November 2001. This additional flux was noted later, as noted in the legend of Fig. 3. We infer that the flux at each moment depended on the shock properties and the fluctuating IMF polarity at the COBpoint as the shock moved outward through the inner heliosphere. Note, in Fig. 3, the instrument saturation from midday on 5 November until early 6 November, the period of time when the shock-associated energetic particle population arrived at the ACE spacecraft.

As noted in Sec. II, the optical flare location, which serves as a proxy for identifying the source of the disturbance, was located at W 23° relative to the sun–Earth line. Figure 4 shows, schematically, plots of predicted flux of 1-MeV protons at a series of observation points (from Aran et al.[12]). Earth's longitude during the 4 November 2001 event corresponds to the location of the predicted flux profile shown in the plot labeled W 22.5°. This plot, albeit computed for a lower particle energy than observed by ACE/SIS during this event, is at least qualitatively representative of the observed flux profiles shown in Fig. 3. The other panels in Fig. 4 represent the flux that would be observed at other 1-AU points in space relative to the sun–Earth line.

In the case just outlined, it is of interest to note that Mars was located about 52° eastward of the sun–Earth line. The event (and inferred shock center line) would have been seen at W 75° from a Martian observer's viewpoint. The COBpoint for an observer located at 1.5 AU is different from the corresponding one at 1 AU (depending on the solar wind velocity). We suspect that some of the spontaneous computer reboots experienced during 3–6 November 2001 by the Mars orbiter camera instrument orbiting Mars (J. Kappenmann, Metatech Corp., private communication, 2002) on board the Mars global surveyor were caused by these particles. The underlying physics and operational tools are described, respectively, by Lario et al.[10] and Sanahuja et al.[11]

IV. Conclusions

We have described a first-generation operational scheme that provides the key links from the sun to the Earth (or elsewhere in the heliosphere) toward the fairly successful prediction of shock arrivals from solar disturbances. This self-consistent approach strongly suggests that it will also be possible to predict the temporal series of other solar wind plasma and IMF parameters in the heliosphere. These predictions would encompass large-scale segments of quasi-steady (nonevent) and disturbed (event) conditions in the space environments outside planetary bow shocks. This linkage, from the sun to the magnetosphere, must be followed by other key links; that is, by other key links that consider additional physics through the Earth's bow shock and energy transport through the magnetopause and still further down to the ionosphere and neutral atmosphere.

Our discussion has focused on a kinematic model, Hakamada–Akasofu–Fry version 2 (HAFv.2). Nearly 400 cases of solar flares and their metric type II radio drifts were considered and communicated to a large group of scientific and operational users in real time via an email listserver distribution (URL: http://gse.gi.alaska.edu/mailman/listinfo/gse-ff). These exercises took place on a continuous basis during solar cycle 23 (February 1997–September 2002). We have presented statistics for shock arrival time forecasts in terms of contingency tables, rms errors for predictive hits, and several skill scores. We have also discussed the use of the HAFv.2 model (and, by implication, more advanced three-dimensional magnetohydrodynamical numerical models) for the determination of additional plasma and IMF parameters. This approach enables predictions of shock-accelerated energetic particle fluxes and fluences at arbitrary positions in the heliosphere, including Earth and outward-bound space missions to Mars and elsewhere.

Acknowledgments

This study was partially funded by the University Partnering of Operational Support program (UPOS), sponsored jointly by the U.S. Air Force and U.S. Army (CDF, MD, WS, CSD, and SIA). This work was also partially funded under NASA Living With a Star (LWS) Targeted Research and Technology Grant NAG5-12527 (CDF, MD) and NOAA Work Order W-10,118(ZS, TRD); by ESA-ESTEC Contract 14098/99/NL/MM to the University of Barcelona (AA, BS); and by NASA Grant NAG5-10787 (DL). Solar radio, optical, and x-ray event data were provided by the National Solar Observatory, the U.S. Air Force, and NOAA. Additional solar radio data were provided by the Culgoora Solar Observatory, Ionospheric Prediction Service, Australia, and the IZMIRAN (Institute of Terrestrial Magnetism, Ionosphere and Radiowave Propagation) Solar Radio Laboratory, Russia. We are grateful to the Wind spacecraft team for solar wind data provided by the SWE (K. Ogilvie) and MFI (R. Lepping) instruments and to the ACE team for solar wind, IMF, and energetic particle data provided by the MAG (N. F. Ness), SWEPAM (D. J. McComas) and SIS (R. A. Mewaldt) instruments. M. Kartalev, D. Berdichevsky, and C. Smith graciously provided some of the shock determinations used in this study. MD thanks the NOAA/Space Environment Center for their hospitality.

References

[1] *The Sun to the Earth—And Beyond: A Decadal Research Strategy in Solar and Space Physics*, Solar and Space Physics Survey Committee, Committee on Solar and Space Physics, Space Studies Board, Div. on Engineering and Physical Sciences, National Research Council of the National Academies, National Academies Press, Washington, DC, 2003.

[2] Akasofu, S.-I., "Predicting Geomagnetic Storms as a Space Weather Project," *Space Weather*, edited by P. Song, H. J. Singer, and G. L. Siscoe, AGU Geophysical Monograph, Vol. 125, American Geophysical Union, Washington, DC, 2001, pp. 329–337.

[3] Fry, C. D., Sun, W., Deehr, C., Dryer, M., Smith, Z., Akasofu, S.-I., Tokumaru, M., and Kojima, M., "Improvements to the HAF Solar Wind Model for Space Weather Predictions," *Journal of Geophysical Research*, Vol. 106, No. A10, 2001, pp. 20,985–21,001.

[4] Dryer, M., "Interplanetary Studies: Propagation of Disturbances Between the Sun and Magnetosphere," *Space Science Review*, Vol. 67, No. 3/4, 1994, pp. 363–419.

[5] Dryer, M., "Multidimensional Magnetohydrodynamic Simulation of Solar-Generated Disturbances: Space Weather Forecasting of Geomagnetic Storms," *AIAA Journal*, Vol. 36, No. 3, 1998, pp. 365–370.

[6] Sun, W., Akasofu, S.-I., Smith, Z. K., and Dryer, M., "Calibration of the Kinematic Method of Studying the Solar Wind on the Basis of a One-Dimensional MHD Solution and a Simulation Study of the Heliosphere Between November 22–December 6, 1977," *Planetary and Space Science*, Vol. 33, No. 8, 1985, pp. 933–943.

[7] Manoharan, P. K., Ananthakrishnan, S., Dryer, M., Detman, T. R., Leinbach, H., Kojima, M., Watanabe, T., and Khan, J., "Solar Wind Velocity and Normalized Scintillation Index from Single Station IPS Observations," *Solar Physics*, Vol. 156, No. 2, 1995, pp. 377–393.

[8] Janardhan, P., Balasubramanian, V., Ananthakrishnan, S., Dryer, M., Bhatnagar, A., McIntosh, P. S., "Travelling Interplanetary Disturbances Using Interplanetary Scintillation at 327 MHz," *Solar Physics*, Vol. 166, July 1996, pp. 379–401.

[9] McKenna-Lawlor, S. M. P., Dryer, M., Smith, Z., Kecskemety, K., Fry, C. D., Sun, W., Deehr, C. S. D., Berdichevsky, D., Kudela, K., and Zastenker, G., "Arrival Times of Flare/Halo CME Associated Shocks at the Earth, and Comparison of the Predictions of Three Numerical Models with These Observations," *Annales de Geophysique*, Vol. 20, No. 7, 2002, pp. 917–935.

[10] Lario, D., Sanahuja, B., and Heras, A. M., "Energetic Particle Events: Efficiency of Interplanetary Shocks as 50 keV < E < 100 MeV Proton Accelerators," *Astrophysical Journal*, Vol. 509, No. 1, 1998, pp. 415–434.

[11]Sanahuja, B., Aran, A., Domingo, V., Ortiz, A., and Lario, D., "An Engineering Model for Solar Energetic Particles in Interplanetary Space," Final Rept., ESA-ESTEC Contract 14098/99/NL/MM to Univ. of Barcelona, 2001.

[12]Aran, A., Sanahuja, B., and Lario, D., "How to Get SEP Flux Profiles at 0.4 AU and 1.0 AU," *Proceedings of "Solar Encounter: The First Solar Orbiter Workshop,"* ESA SP-493, Noordwijk, The Netherlands, 2001, pp. 157–170.

[13]Wang, Y.-M., and Sheeley, N. R., "Solar Wind Speed and Coronal Flux-Tube Expansion," *Astrophysical Journal*, Vol. 355, June 1990, pp. 726–732.

[14]Arge, C. N., and Pizzo, V. J., "Improvement in the Prediction of Solar Wind Conditions Using Near-Real-Time Solar Magnetic Field Updates," *Journal of Geophysical Research*, Vol. 105, No. A5, 2000, pp. 10,465–10,479.

[15]Sun, W., Dryer, M., Fry, C. D., Deehr, C. S., Smith, Z., Akasofu, S.-I., Kartalev, M. D., and Grigorov, K. G., "Real-Time Forecasting of ICME Shock Arrivals at L1 During the 'April Fool's Day' Epoch: 28 March–21 April 2001," *Annales de Geophysique*, Vol. 20, No. 7, 2002, pp. 937–945.

[16]Fry, C. D., Dryer, M., Deehr, C. S., Sun, W., Akasofu, S.-I., and Smith, Z., "Forecasting Solar Wind Structures and Shock Arrival Times Using an Ensemble of Models," *Journal of Geophysical Research*, Vol. 108, No. A2, 2002, 1070.doi 10.1029/2002JA009474.

[17]Dryer, M., Fry, C. D., Sun, W., Deehr, C. S., Smith, Z., Akasofu, S.-I., and Andrews, M. D., "Prediction in Real Time of the 2000 July 14 Heliospheric Shock Wave and Its Companions During the 'Bastille' Epoch," *Solar Physics*, Vol. 204, No. 1/2, 2001, pp. 267–286.

C. Kaplan
Associate Editor